Journal of Electronic Materials, Vol. 2, No. 2, 1973

EPITAXIAL GROWTH AND PIEZOELECTRIC PROPERTIES OF AlN, GaN, AND GaAs ON SAPPHIRE OR SPINEL

M. T. Duffy, C. C. Wang, G. D. O'Clock Jr., S. H. McFarlane III, and P. J. Zanzucchi

Abstract

Heteroepitaxial films of the III-V compounds, AlN, GaN and GaAs have been grown on insulating substrates by reactions involving Group III metal-organic compounds and Group V hydrides. The films were examined with respect to crystallography, surface topography, uniformity, residual strain, and electrical and acoustic properties with emphasis on those orientations which are of particular interest to surface acoustic wave (SAW) device applications. Aluminum nitride films up to 10 μm in thickness were grown on 1" diameter sapphire substrates with a 5% to 10% thickness variation. The films, though characterized as single crystal by x-ray means, exhibited a grain-like structure and considerable surface faceting. The residual strain in the films depends on the crystallographic direction and increases substantially with film thickness. These films exhibit useful surface acoustic properties. Epitaxial GaN films are more easily prepared than AlN films but by contrast are semiconducting unless "doped" with Zn or Li during the growth process. Films of this material are similar crystallographically to AlN and preliminary results show that they exhibit piezoelectric properties. The lack of published data on the acoustic properties of GaN films is probably due to the difficulty in compensating the films to provide insulating layers in device structures. Preliminary results obtained on GaAs epitaxial layers are discussed briefly because of the semiconducting properties of this material.

Research jointly sponsored by the Air Force Materials Laboratory, Wright-Patterson Air Force Base, under Contract F33615-70-C-1536 and RCA Laboratories, Princeton, N. J. and by RCA Advanced Technology Laboratories-West, Van Nuys, California
Received 6 December 1972; revised 12 February 1973.

© 1973 by the American Institute of Mining, Metallurgical, and Petroleum Engineers, Inc.

Introduction

The development of surface acoustic wave device technology offers the prospect of attaining a new generation of sophisticated high speed signal processing devices with characteristic reduction in size and complexity relative to their electromagnetic counterparts (1). As compared to bulk wave devices, in which the acoustic wave cannot be modified until it leaves the output, the surface waves are physically accessible and can be tapped, amplified and manipulated along the entire propagation path. These considerations have given much impetus to the study of SAW (surface acoustic wave) devices for several applications during the past few years. To realize the full potential of surface waves in practical device geometries the materials preparative techniques must be advanced in order to combine materials with specific functional properties in composite structures which are not yet available. Such structures would attempt to combine piezoelectric materials for transducers, low loss materials for transmission and delay lines, and semiconducting materials for amplification. The realization of composites of this nature should lead not only to the optimization of discrete SAW devices, but also to compatible interfacing of SAW structures with the highly developed and versatile MOS/LSI (metal-oxide-semiconductor/large scale integration) circuitry to provide an electronically programmable integrated SAW technology.

The preparative problems associated with the realization of this goal are particularly complex because of the specific requirements imposed on the crystalline nature and properties of the materials involved. An additional constraint is imposed by the condition that the signal must be transferred from one processing function to another while maintaining materials continuity, i.e., the various crystalline materials must preferably be on the same substrate. These conditions have limited progress in the monolithic approach to an integrated SAW technology. In recent years, however, the achievement of heteroepitaxial growth of several piezoelectric materials such as ZnO, AlN, GaN, and GaAs on low loss insulating substrates such as sapphire and spinel (2-19) with desired crystallographic orientations, which are also compatible with the present silicon-on-sapphire (SOS) technology (20), has enhanced progress in attaining the objective outlined. This paper reports the results of preliminary measurements made on three piezoelectric materials (AlN, GaN, and GaAs) which were grown epitaxially on insulating substrates (sapphire and/or spinel), and which are of interest to the development of an integrated SAW technology.

Experimental

Film Growth Process. Single crystal films of AlN, GaN, and GaAs were grown on sapphire and/or spinel substrates utilizing the metal-organic-hydride reactions (7,12) indicated in Table I. The metal-organic reagents are pyrophoric liquids at room temperature and are obtained in stainless steel containers equipped with a central dip tube and side port to enable the transport of the vapors to the reaction chamber by bubbling a suitable gas such as hydrogen through the liquid. The rate of transport can be controlled by controlling the temperature

Table I. Epitaxial Growth Process

Epitaxial Material System	Growth Process
(1) AlN on sapphire	Reaction between $(CH_3)_3Al$ and NH_3.
(2) GaN on sapphire	Reaction between $(CH_3)_3Ga$ and NH_3. Zn or Li doping during growth process to provide insulating films.
(3) GaAs on sapphire (and spinel)	Reaction between $(CH_3)_3Ga$ and AsH_3.

of the liquid and the flow rate of the transporting gas. The hydride is introduced as gaseous NH_3 from a cylinder of liquid ammonia, or as AsH_3 in hydrogen ambient in the case of GaAs films. Schematics of the epitaxial growth apparatus are presented in Figure 1 and reference (14). In the case of AlN and GaN films the reactants enter the reaction chamber by separate ports and are not allowed to mix until reaching the vicinity of the heated substrate in order to minimize the formation of intermediate compounds which form upon mixing even at lower temperatures (7). Previous studies utilized a central vertical delivery tube with various orifice cross-sections for the transport of the metal-organic vapors to the reaction zone (7). Because of the high substrate temperatures employed, particularly in the case of AlN films, strong convection currents interfere with the delivery gas flow pattern resulting in very nonuniform layers as evidenced by the many visible interference fringes exhibited by the films. In order to overcome these problems, the system depicted in Figure 1 utilizes a delivery tube which is offset to the side of the reaction chamber. In this manner the vapors tend to follow the path of the convection currents and much more uniform films can be obtained over larger areal dimensions. In the case of GaAs films, separate delivery of the reactants is not necessary and such precautions can be eliminated. In all cases excess hydride is used since this contains the element which is likely to be deficient in III-V compounds.

The quartz reaction chamber has an inner diameter of 6.5 cm and is 15 cm in length. The side delivery tube is made of quartz and has an inner diameter of approximately 0.4 cm. The exit orifice has similar dimensions and is oriented so that the gases are projected across and downwards over the rotating substrate. The rotary shaft carrying the substrate and silicon carbide coated susceptor is raised and lowered during the growth process so that the gases are projected toward different parts of the substrate (see Figure 1) in order to enhance uniformity. The vertical separation between orifice and substrate is varied from about 0.2 cm to 2.0 cm.

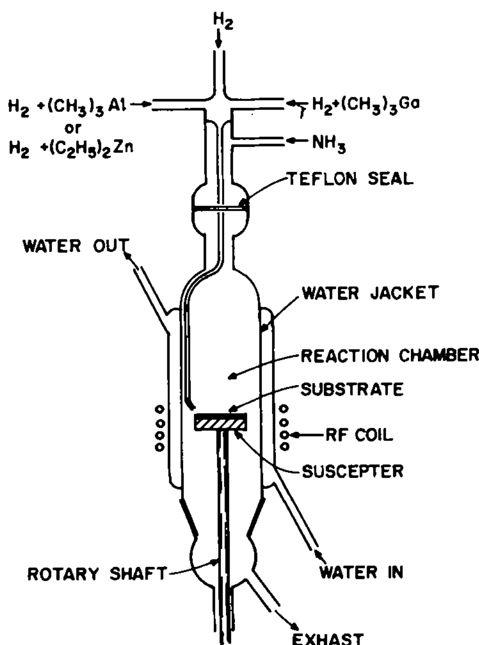

Figure 1. Apparatus for AlN and GaN epitaxy.

Hydrogen flow rates through the side delivery tube were maintained in the range 4.0 l/min to 6.5 l/min in the case of AlN films, and at 4.0 l/min in the case of GaN films. Palladium diffused hydrogen was used throughout. The metal-organic vapors were transported to the main hydrogen stream by bubbling hydrogen through the respective containers at 20°C in the case of the less volatile liquids. This flow rate was 1 ml/min through $(CH_3)_3Al$ (6N Electronic Grade, v.p. $\simeq$ 8 mm at 20°C) during the formation of AlN. The vapor pressure of $(CH_3)_3Ga$ (6N Electronic Grade, v.p. $\simeq$ 175 mm at 20°C) is relatively high and the vapors were permitted to diffuse into the main stream of hydrogen without the aid of a transporting gas during the growth of GaN films. In order to increase the resistivity of GaN, zinc dopant was introduced during the growth process by transporting the vapors of $(C_2H_5)_2Zn$ (5N Electronic Grade, v.p. $\simeq$ 15 mm at 20°C) in a hydrogen flow of 5 ml/min. The flow rate of NH_3 (5N Electronic Grade) was 2.5 l/min in all cases. The temperature range for the growth of AlN was 1200°C to 1250°C, and 750°C to 1100°C for the growth of GaN.

Lithium was also used as dopant during the growth of GaN. The lithium source was provided by heating LiOH in air on a silicon carbide coated susceptor until molten at about 450°C. The liquid spread uniformly over the susceptor and was then heated at somewhat higher temperatures until dehydration was complete and a white powdery coating remained. The temperature was then raised to about 1100°C for approximately 15 min before finally cooling to room temperature. This provided the lithium source when growth was performed using the same

susceptor. Alternatively, the source may be prepared in a separate crucible and the powders collected and heated in the vicinity of the growing film. Both powder and initial hydroxide are corrosive, and important surfaces such as those of sapphire and the piezoelectric film should be protected from direct contact at high temperatures.

The substrates used were sapphire, spinel and silicon and were cleaned ultrasonically in solvents prior to the growth process. In many cases the refractory substrates were also air annealed and chemically etched (21) in order to minimize surface polishing damage. Several substrate orientations were used, but this paper will be confined to those orientations which are pertinent to SAW device technology and/or exhibit preferential epitaxial relationships in relation to overlay crystal growth, and will be discussed in the next section. Substrate orientations were cut to within 1/2°.

The growth rate for AlN heteroepitaxy was 1 μm to 3 μm per hour corresponding to the flow rates given above, and 3 μm per hour for the growth of GaN. The apparatus and growth conditions for GaAs heteroepitaxy have been described previously (14,17,19).

Results and Discussion

Film Properties. Epitaxial AlN films ranging in thickness up to 10 μm were grown on (01$\bar{1}$2)-oriented and (0001)-oriented sapphire, and on (111)-oriented silicon substrates. The films were characterized by Laue back-reflection and diffractometry x-ray techniques and were found to exhibit single crystal character with the following epitaxial relationships:

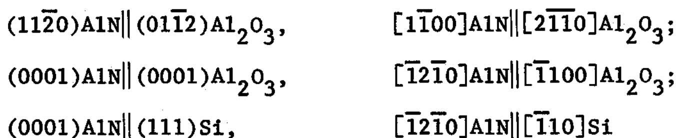

$(11\bar{2}0)AlN \| (01\bar{1}2)Al_2O_3$, $[1\bar{1}00]AlN \| [2\bar{1}\bar{1}0]Al_2O_3$;

$(0001)AlN \| (0001)Al_2O_3$, $[\bar{1}2\bar{1}0]AlN \| [\bar{1}100]Al_2O_3$;

$(0001)AlN \| (111)Si$, $[\bar{1}2\bar{1}0]AlN \| [\bar{1}10]Si$

as previously reported (7). Films too thin for x-ray analysis were characterized by electron diffraction and the above relationships verified. Most experiments were performed with (01$\bar{1}$2)-oriented sapphire substrates since the (11$\bar{2}$0)-oriented epitaxial AlN layer contains the c-axis of its hexagonal structure in the plane of the film. Acoustic propagation along this axis has been the subject of previous studies (22,23). The same sapphire orientation appropriately serves as substrate orientation for silicon-on-sapphire (SOS) heteroepitaxy. Films grown on silicon substrates were invariably cracked or crazed at film thicknesses greater than about 0.4 μm.

As-grown AlN films on both sapphire and silicon substrates exhibit interesting surface topography. Scanning electron micrographs of 10 μm thick films on (01$\bar{1}$2)-oriented sapphire and (111)-oriented silicon are presented in Figure 2. It can be seen from the micrographs and the epitaxial relationships given above that surface crystallites are aligned in parallel fashion with their axes parallel to the c-axes of

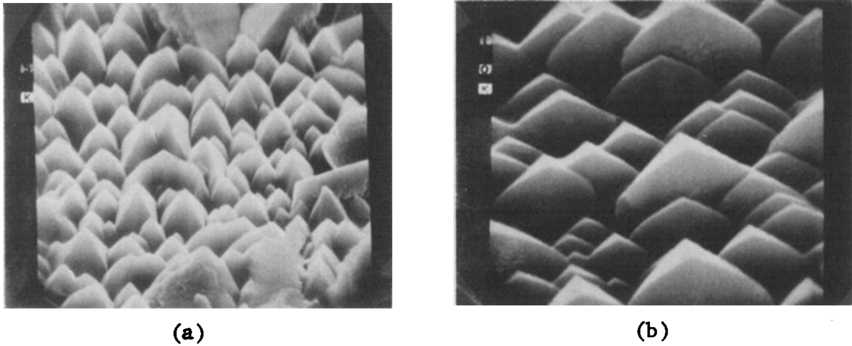

(a) (b)

Figure 2. Scanning electron micrographs of AlN films (~10 μm) on (a) (111) silicon substrate; AlN c-axis is perpendicular to plane on film, (b) (01$\bar{1}$2) Al_2O_3 substrate; AlN c-axis is in plane of film.

the films. Since smooth optical quality surfaces are required for the fabrication of interdigital transducer patterns for SAW measurements, the films were mechanically polished using the finest grade of "Linde" (0.05 μ). This was followed by chromium oxide polishing which appears to provide more scratch-free surfaces suitable for fine patterning photolithography. Polished films show a grain-like structure, the grain size increasing with film thickness. This might be expected from the electron micrograph of Figure 2 and reported work on other III-V compounds (17).

A consideration of importance to the device engineer in the study of SAW materials is the uniformity and areal extent of the films. As already stated, it is difficult to meet these requirements because of the high temperature (~1200°C) associated with AlN heteroepitaxy. This is further complicated by the requirement of uniform surface polishing. Thickness profiles of two polished AlN samples (1" diameter) are presented in Figure 3. Measurements were made at 0.1" intervals by an infrared interference technique (24). The direction chosen was arbitrary since rotation of the substrate during the growth process favors circular symmetry in film thickness. The final surface profile after polishing tends to follow the original surface contour, as can be seen from the variation in film thickness. The two thickness profiles shown correspond to two different flow rates through the side delivery tube of Figure 1 (top curve: 6.5 l/min; bottom curve: 4.0 l/min). The final thickness uniformity can be controlled to between 5% and 10% over a 1" diameter film.

Another aspect of concern in the epitaxial process is the residual strain in the grown films. It is conceivable that this could modify many of the properties of a film with respect to the bulk crystalline properties of the same material. Results of the present investigation indicate that the strain in AlN films becomes excessive at thicknesses

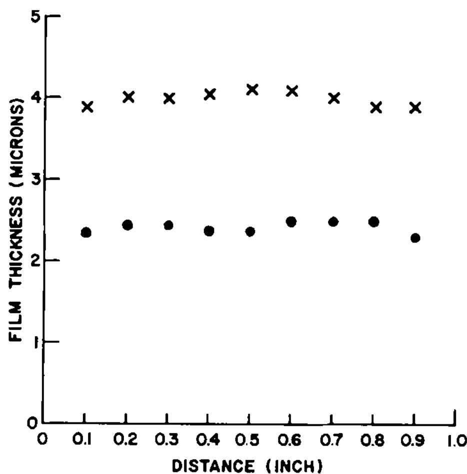

Figure 3. Thickness profiles obtained by an infrared technique on two polished AlN samples (1" dia.). Measurements were made at 0.1" intervals, beginning 0.1" from edge. The direction chosen was arbitrary; because the substrate is rotated during film growth, circular symmetry in relation to thickness is usual.

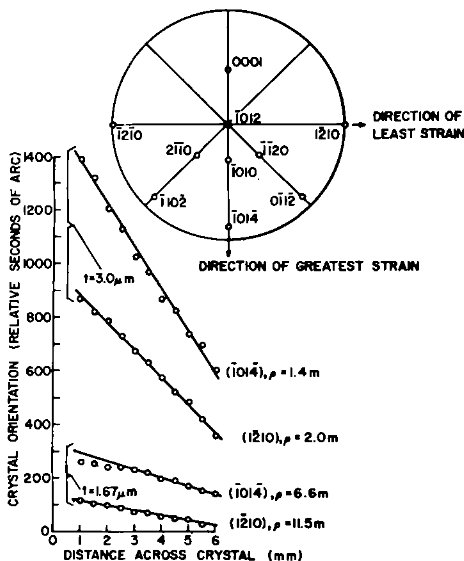

Figure 4. Change in angular setting of a sapphire substrate for a particular reflection as a function of distance across the Al_2O_3 crystal for each of two AlN/Al_2O_3 structures. The radius of curvature, ρ (meters), is indicated along two perpendicular directions for each of two samples of thickness, t, 1.67 μm and 3.0 μm, respectively.

above about 4 μm. In some cases films were observed to shatter when subjected to relatively small temperature gradients or mechanical stress for film thicknesses in the range 5-10 μm. Figure 4 shows the curvature resulting from residual strain in two AlN/sapphire structures along two perpendicular zones as indicated in the inset stereographic projection. The curvature of each substrate was determined by an x-ray technique (17) in which the angular setting of the substrate corresponding to the Bragg condition for reflection from selected planes [($\bar{1}01\bar{4}$) and ($1\bar{2}10$)] is determined as a function of substrate displacement. Since the structures are curved, the reflecting crystallographic planes are no longer parallel, and the deviation relative to the initial measurement at an edge of the substrate is recorded as relative seconds of arc versus horizontal translation of the substrate as presented in Figure 4. The slope of the curve is inversely proportional to the radius of curvature, ρ (given in meters), of the crystal. If the strain is isotropic, the substrate curvature is independent of the direction of measurement across the substrate. It can be seen that the strain is

anisotropic as might be expected for the orientations involved [(11$\bar{2}$0)AlN/(01$\bar{1}$2)sapphire] because of differences in the elastic and thermal expansion properties of both film and substrate with respect to their different crystallographic directions. The strain in the films increases substantially with film thickness, as can be seen from the decrease in the value of ρ for a given direction of measurement when the film thickness, t, is increased from 1.67 μm to 3.0 μm. The strain is such that the contraction of the substrate upon cooling forces the film into compression and deforms the film-substrate composite making the film side convex.

As-grown AlN films were insulating and unlike GaN and ZnO films on sapphire (2,26,27) require no diffusion of dopants to provide sufficiently high resistivities for SAW applications.

Epitaxial GaN films ranging in thickness up to several tens of microns were grown on sapphire substrates with the same orientation relationships as discussed in the case of AlN and were characterized in similar fashion. Films grown on silicon were polycrystalline. The substrates used most frequently were (01$\bar{1}$2)-oriented sapphire and growth temperatures in the range 800°C to 1100°C were investigated. In all cases the films were semiconducting (n-type) with typical electrical properties as shown by the range in Table II for undoped films. The mobilities shown here are lower than those reported for thicker films prepared by the chloride vapor transport technique (27), but are in agreement with those reported in reference (7) by the same preparative technique.

Since high resistivity material is required for transducer application, various attempts were made to compensate GaN films during the growth process with Zn (27) using the vapors of diethyl zinc as source material (see Figure 1). It was found that at the higher growth temperatures only a partial compensation of GaN occurred, while at the lower temperatures resistivities in the range 10^6-10^8 Ω-cm could be obtained (see Table II). It is interesting to note that no deterioration in crystalline character based on x-ray analysis and electrical properties resulted from the lower growth temperature. An alternative approach to obtaining high resistivity GaN films was tested using lithium as the compensating element during the growth process. It was found that insulating films were readily obtained at all growth temperatures in the range tested (800°C to 1100°C). The lithium was found optically to occupy a deep energy level at approximately 2.2 eV. Similar properties were reported (28) for GaN crystals prepared with starting materials containing lithium.

Gallium nitride films exhibit similar structure to that of aluminum nitride but are more readily prepared with good thickness uniformity and more easily polished. The residual stress in the films was also found to be less than in the case of AlN.

The properties of GaAs films grown on insulating substrates (sapphire and spinel) by the reaction indicated in Table I are too encompassing to treat here and are treated in separate papers (14,16,17,19).

Table II. Electrical Properties of GaN and AlN Epitaxial Layers

Composite	Growth Temp. °C	Film Thickness μm	Carrier Conc. cm^{-3}	Resistivity Ω-cm, n-type	Hall Mobility cm^2/V-sec
$(11\bar{2}0)$GaN/ $(01\bar{1}2)Al_2O_3$	1050	2.8	$1x10^{19}$	0.017	55
$(11\bar{2}0)$GaN/ $(01\bar{1}2)Al_2O_3$ (Zn-doped)	1050	2.2	$4x10^{17}$	0.306	51
$(11\bar{2}0)$GaN/ $(01\bar{1}2)Al_2O_3$	850	4.8	$3x10^{19}$	0.003	75
$(11\bar{2}0)$GaN/ $(01\bar{1}2)Al_2O_3$ (Zn-doped)	850	5.0	--	insulating	--
$(11\bar{2}0)$AlN/ $(01\bar{1}2)Al_2O_3$	~1200	--	--	insulating	--

This material offers interesting possibilities in microsonics because of its combined piezoelectric and semiconducting (high electron mobility) properties.

Acoustic Properties. Several electro-acoustic properties are related to the structural properties of the various epitaxial composite material systems. In general, surface wave properties are highly dependent upon the plane and direction of propagation (29), on the epitaxial layer thickness and acoustic properties of the substrate (30-32). In order to optimize the properties of the piezoelectric films, it is necessary to correlate several acoustic properties relating to the generation, propagation and detection of acoustic surface waves with the synthesis parameters. To make acoustic measurements, high resistivity films of AlN and GaN with polished surfaces were equipped with metallized interdigital input-output transducer patterns and surface waves generated and detected in the usual manner (1). The interdigital patterns were arranged so that acoustic propagation occurred along the "c" axis of each film in the case of $(11\bar{2}0)$-oriented films and independent of direction in the case of (0001)-oriented films. Properties such as surface wave velocity, V_s, insertion loss, L_i, propagation loss, L_p, transducer capacitance, C_t, and fractional velocity change $\Delta V/V$ were then measured and preliminary values are presented in Table III. The transducer patterns were chrome-gold with a center to center finger spacing of 29 μm and the transducer aperture was 3 mm. The number of finger pairs per pattern was 6.

Table III. Electro-Acoustic Characteristics of SAW Epitaxial Materials

SAW Material	Configuration and Thickness/Wavelength Ratio	V_s ($\times 10^5$ cm/s)	L_i dB	L_p dB/μsec	C_t pf	ΔV/V	f MHz
GaAs	18 μm (111) GaAs on (111) spinel. $t/\lambda = 0.62$	2.75		~0.1			95
AlN	2.74 μm (11$\bar{2}$0) AlN on (01$\bar{1}$2) sapphire. $t/\lambda = 0.04$	6.05	25	~0.1	2.5	0.003	101
AlN	10.0 μm (11$\bar{2}$0) AlN on (01$\bar{1}$2) sapphire. $t/\lambda = 0.17$	5.9	43	~0.1	2.5	0.00037	98.4
AlN	0.8 μm (0001) AlN on (0001) sapphire. $t/\lambda = 0.012$	6.1		~0.1			95
GaN	1.0 μm (0001) GaN on (0001) sapphire. $t/\lambda = 0.016$	5.75	55	~0.1	2.6	0.0001	95

The GaAs films tested were semiconducting and alternative means of coupling acoustically to the films was necessary. The experimental procedure involved coupling surface waves from a $LiNbO_3$ substrate to the gallium arsenide surface utilizing a fluid layer between the two surfaces to enhance mechanical coupling (33). The values obtained are also presented in Table III. Figures 5 and 6 show the input signal and time delayed output pulse for AlN and GaN films listed in this Table, while Figure 7 shows the corresponding detail for the case of a GaAs film. The GaAs film referred to in Figure 7 and Table III was grown on (111)-oriented spinel and the film thickness was 18 μm. The film was characterized electrically as n-type, 0.6 ohm-cm, with a carrier concentration of $4.0\times10^{15}/cm^3$ and a Hall mobility of 2680 cm^2/V-sec.

The thickness to wavelength ratios (t/λ) indicated in Table III are less than unity. Consequently, acoustic properties such as surface wave velocity will depend upon film thickness as can be seen from the data on AlN films. No information is yet available on the acoustic properties of films of these materials for $t/\lambda > 1$ because of the difficulty in preparing suitable epitaxial layers in the appropriate thickness range. It should be noted that the results given in Table III do not represent optimized values with respect to film preparation and device fabrication, and loss values such as insertion loss, L_i, can be expected to decrease significantly with optimization.

The values of the electromechanic coupling coefficient (k^2) of AlN films calculated from the data ($k^2 \approx 2$ $\Delta V/V$) in Table III are in good agreement with previously published values for films in the 1 μm to 2 μm thickness range (22). However, a direct comparison is not possible for thicker epitaxial films because of the lack of reported data.

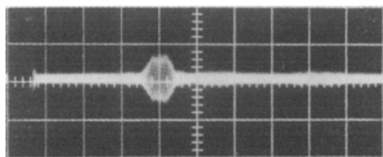

Figure 5. Input pulse and time-delayed output pulse characteristics for GaN/Al_2O_3 composite referred to in Table III. (3.7 μsec over 2.13 cm GaN surface.) (Vertical: 0.5 V/division.)

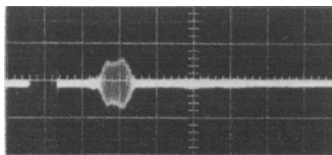

Figure 6. Input pulse and time-delayed output pulse characteristics for AlN/Al_2O_3 composite referred to in Table III (film thickness: 0.8 μm). (1.8 μsec over 1.1 cm AlN surface.) (Vertical: 0.5 V/division).

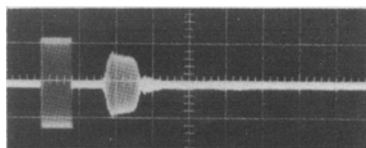

Figure 7. Input pulse and time-delayed output pulse characteristics for $GaAs/MgAl_2O_4$ composite referred to in Table III. (6.8 μsec over 1.9 cm GaAs surface.) (Vertical: 0.5 V/division.)

Not enough information is available on GaN epitaxial layers at this time to draw a comparison with AlN films. These films have, however, been found to exhibit piezoelectric properties.

Gallium arsenide films are only weakly piezoelectric but have high electron mobility and low acoustic surface wave velocity. These latter properties make GaAs a potentially useful waveguide and amplification medium.

Conclusions

Heteroepitaxial III-V compound films, AlN, GaN, and GaAs on insulating substrates exhibit promising characteristics for application in surface acoustic wave device technology. The surface wave velocity on AlN films is almost double that on the better known piezoelectric materials such as quartz and lithium niobate, thus enabling a corresponding increase in the device operating frequency for a given transducer pattern geometry.

Gallium nitride films, though studied optically (34), have not been characterized previously with respect to their piezoelectric properties insofar as we are aware. This probably has been due in large measure to the difficulty in obtaining sufficiently high resistivity films for measurements. The results obtained here show that insulating GaN films can readily be prepared under appropriate conditions and that the films are piezoelectric with interesting properties for potential device application. However, extensive studies are still required to determine the merits of this material relative to AlN.

Gallium arsenide films exhibit high electron mobility and low surface wave velocity, factors of considerable importance to the wave-guiding and amplification of surface acoustic waves.

Acknowledgments

The authors wish to thank R. T. Smith for x-ray analysis, J. Mitchell for photolithography, J. I. Pankove for optical measurements, B. Seabury for electron microscopy, E. A. Miller and F. Dougherty for Hall mobility measurements, and R. A. Soltis for technical assistance.

References

1. For a review see:
   P. H. Carr, IEEE Trans. on Microwave Theory and Tech. MTT-17, 845 (1969).
   E. Stern, ibid., 835 (1969).
   D. A. Gandolfo, RCA Engineer 15, 54 (1969).
   R. M. White, Proc. IEEE 58, 1238 (1970).

2. G. Galli and J. E. Coker, Appl. Phys. Letters 16, 439 (1970).

3. J. H. Collins, P. J. Hagon, and G. R. Pulliam, Ultrasonics 8, 218 (1970).

4. J. M. Hammer, D. J. Channin, M. T. Duffy, and J. P. Wittke, Appl. Phys. Letters 21, 358 (1972).

5. A. J. Noreika and D. W. Ing, J. Appl. Phys. 39, 5578 (1968).

6. G. A. Cox et al., J. Phys. Chem. Solids 28, 543 (1967).

7. H. M. Manasevit, F. M. Erdmann, and W. I. Simpson, J. Electrochem. Soc. 118, 1864 (1971).

8. W. M. Yim, E. J. Stofko, P. J. Zanzucchi, J. I. Pankove, M. Ettenberg, and S. L. Gilbert, J. Appl. Phys. 44, 292 (1973).

9. B. B. Kosicki and D. Kahng, J. Vacuum Sci. Technol. 6, 593 (1969).

10. H. P. Maruska and J. J. Tietjen, Appl. Phys. Letters 15, 327 (1969).

11. D. K. Wickenden et al., J. Crystal Growth 9, 158 (1971).

12. H. M. Manasevit and W. I. Simpson, J. Electrochem. Soc. 116, 1725 (1969).

13. P. Rai-Choudhury, J. Electrochem. Soc. 116, 1745 (1969).

14. C. C. Wang and S. H. McFarlane III, J. Crystal Growth 13-14, 262 (1972).

15. H. M. Manasevit and W. I. Simpson, J. Electrochem. Soc. 118, 644 (1971).

16. A. C. Thorsen and H. M. Manasevit, J. Appl. Phys. 42, 2519 (1971).

17. S. H. McFarlane III and C. C. Wang, J. Appl. Phys. 43, 1724 (1972).

18. H. M. Manasevit and A. C. Thorsen, Trans. Met. Soc. AIME 1, 623 (1970).

19. C. C. Wang, Technical Report AFML-TR-72-138, June (1972).

20. G. W. Cullen, J. Crystal Growth 9, 107 (1971).

21. A. Reisman, M. Berkenblit, J. Cuomo, and S. A. Chan, J. Electrochem. Soc. 118, 1653 (1971).

22. P. J. Hagon, L. Dyal, and K. M. Lakin, IEEE Ultrasonics Symposium Proceedings, Boston meeting, Oct. 1972 (page 274).

23. L. R. Adkins, ibid. (page 292).

24. O. S. Heavens, Thin Film Physics, Methuen and Co. Ltd., London (1970).

26. J. I. Pankove, E. A. Miller, D. Richman, and J. E. Berkeyheiser, J. of Luminescence 4, 63 (1971).

27. J. I. Pankove, E. A. Miller, and J. E. Berkeyheiser, RCA Review 32, 383 (1971).

28. H. G. Grimmeiss, R. Groth, and J. Maak, Z. Naturforsch. 15a, 799 (1960).

29. A. J. Slobodnik, Jr. and E. D. Conway, Microwave Acoustics Handbook, Rpt. AFCRL-70-0164 (1970).

30. R. V. Schmidt and F. W. Voltmer, IEEE Trans. on Microwave Theory and Techniques MTT-17, 920 (1969).

31. M. R. Daniel and J. de Klerk, Appl. Phys. Letters 16, 331 (1970).

32. W. R. Smith, J. Appl. Phys. 42, 3016 (1971).

33. P. Das and M. N. Araghi, Appl. Phys. Letters 16, 293 (1970).

34. J. I. Pankove, E. A. Miller, and J. E. Berkeyheiser, J. Luminescence 5, 84 (1972).